SPATIAL PATTERN OF SOIL EROSION USING RUSLE MODEL AND GIS SOFTWARE AT THE SAF SAF WATERSHED, ALGERIA

ZINE EL ABIDINE BOUKHRISSA[1], KAMEL KHANCHOUL*[2], OUAFA OTHMANI[2]

[1, 2] Department of Geology, Soil and Sustainable Development Laboratory, Badji Mokhtar University-Annaba, Algeria
[3] Department of Biology, Soil and Sustainable Development Laboratory, Badji Mokhtar University-Annaba, Algeria
*Email: kam.khanchoul@gmail.com, kamel.khanchoul@univ-annaba.dz

Received 13 January 2022, accepted in revised form 28 February 2022

Abstract
Soil erosion is one of the problems threatening the Algerian environment. In agriculture, soil erosion leads to the thinning of the topsoil under the effect of the natural erosive forces of water, or under the effect of agricultural activities. The present study focuses on analysis and mapping of the vulnerability to water erosion in Saf Saf watershed, Algeria, through the integration of RUSLE model with geographic information system (GIS). Various parameters are utilized such as the rainfall erosivity factor (R), soil erodibility factor (K), slope length - slope steepness factor (LS), crop management factor (C) and practice management factor (P). The results are organized into seven classes of different soil erosion rate values. They have revealed that eighty five percent of the study area is experiencing acceptable rate of soil erosion loss less or equal to 5 t ha^{-1} yr^{-1} with potential soil erosion of 3.29 t ha^{-1} yr^{-1}. The high soil losses are favored by steep slopes and degraded vegetation cover, mainly located in northeast, northwest and south of the basin. The present study of risk assessment can contribute to understand the spatial pattern of soil erosion in order to use appropriate conservation practices for sustainable soil management.

Keywords: Soil erosion; Soil loss; RUSLE; GIS; Saf Saf watershed

1. Introduction

Soil results from the association of a mineralogical support with a colloidal complex of which is an essential element for agricultural production. It consists of complex dynamic processes that depend on many physical factors such as soil type, topography, climatic characteristics, land use, human activities (Teixeira Guerra et al., 2017; Shi et al., 2019). Soil erosion is a natural process that can be slow and go relatively unnoticed. It can also occur at an aggressive rate and then cause heavy losses of arable land, resulting in the decline of ecosystem functions (Angassa, 2014; Haregeweyn et al., 2015). Among other things, intensive use of agricultural land can lead to soil depletion of organic matter, degradation of soil structure and gradual decline in natural soil fertility. When water does not infiltrate and flows on the soil surface, it becomes the main agent

of erosion, causing the transport of soluble soil components including contaminants (FAO, 2015). By considering the mechanism of water erosion, there is the effect of the atmospheric precipitation in dislodging and breaking soil particles into small pieces that will be likely to be entrained by water. Soil aggregates are carried away by runoff, but raindrops, because they possess by kinetic energy, exert, at their point of impact on these previously moistened aggregates, a mechanical effect. They cause detachment of fine particles from the surface and transport them as suspended particles.

The degradation of resources is a very important spatial and temporal phenomenon in many Mediterranean countries. Inadequate agricultural practices can have serious effects on the environment where the soil can be subjected to a series of erosive processes (Panagos et al., 2016c). In Algeria, soil erosion results mainly from the overexploitation of soil resources and the reduction of plant cover. This situation is taking considerable proportions in undeveloped areas. The intense erosion in some vulnerable areas is one of the most distinctive characteristics of the Saf Saf basin, of which one can see siltation in a very advanced state of the Zardezas dam, having an initial capacity of 15 million m^3 and located downstream of the study basin. This dam, built in 1945, is filled at more than 50% of sediments and a technique of raising of the dyke becomes necessary (Khanchoul et al., 2007).

A quantitative assessment is needed to deduce the extent of surfaces affected by soil erosion in order to realize soil conservation strategies. However, the complexity of the factors involved makes it difficult to accurately predict erosion. Developments in spatial technologies and Geographic Information Systems (GIS) have improved the existing methods and provided effective models for measuring and analyzing the phenomenon of erosion at watershed scales. Digital Elevation Model input along with remote sensing data, GIS and suitable physical factors (geology, terrain morphology, soil type and climate) can help to determine and model soil erosion hazards in watersheds (Kouli et al., 2009; Prasannakumar et al., 2012; Ganasri, and Ramesh, 2016).

Several models have been developed to estimate soil erosion risk, in that most commonly used models are the Universal Soil Loss Erosion (USLE) and its revised version (RUSLE) developed by Wischmeier, and Smith (1965) and Renard et al. (1997) respectively. The RUSLE incorporates improvements in the factors based on improved new data but keeps the basis of the USLE equation. The combination of GIS with RUSLE technique is now considered being a very reliable and practical models most suited to predict erosion risk with reasonable costs (Fang et al., 2019).

The aim of the present study is to estimate the annual soil loss in the Saf Saf watershed, northeast of Algeria by using RUSLE and geospatial technique. The selected watershed is considered vulnerable to erosion; mainly by high suspended sediment load transport in streams due to weak rock series outcrop existence. In addition, the present study is expected to contribute to the development of appropriate and judicious use of soil and water conservation measures in high risk zones of the river basin.

2. Study area

The Saf Saf watershed is located in the Tell Mountain ridge with an area of 320.17 km^2 at the Khemakhem gauging station (Fig.1). At 6 km downstream, the Zardézas reservoir receives the sediment loads from the Saf Saf basin river. The Saf Saf River is applied from the junction of the Khemakhem Wadi and the Bou Adjeb Wadi. The Saf Saf basin is dominated by high relief and steep slopes that may trigger intense runoff and contribute to soil instability through erosional processes.

The study basin is characterized by several geologic formations from limestone and sandstone to vulnerable rocks to erosion. The Saf Saf watershed has 44% of its area

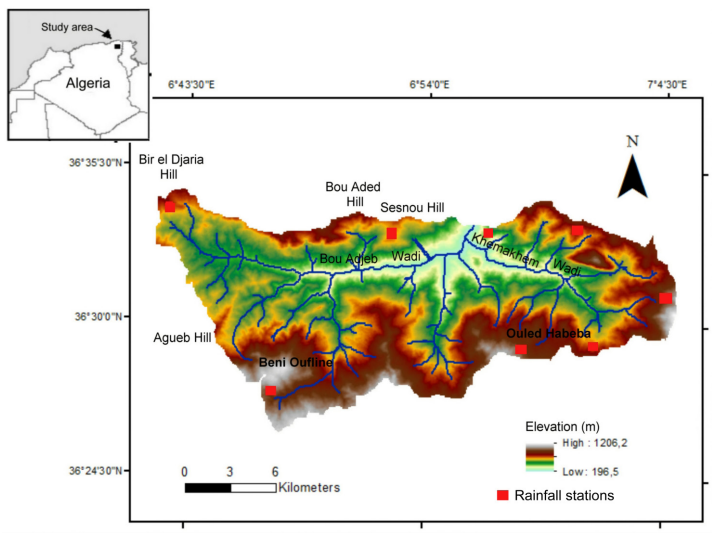

Fig. 1. Location and elevation map of Saf Saf watershed

covered by erodible marly limestone of Senonian, gypseous-sandy clay and clayey conglomerate of continental Miocene and the lower Numidian clay (Khanchoul et al., 2007). Conglomerate formations (with 19% of the basin area) are greatly affected by folds and faults, which show a dense drainage network often in conformity with the geologic structure. The resistant outcrops including limestone and Oligocene sandstone (with 29% of area)are made up of highly dissected hills. The floodplain is less extended and occupies a narrow area along Bou Adjeb and Khemakhem wadis, which are subject to bank erosion.

The basin is composed of four types of soil according to the Constantine soil map and FAO. These are the predominantly Chromic Cambisols, Calcic Cambisols, Orthic Solonetz and Podzolic soils. In the Mediterranean area some Orthic Solonetz are suitable for olive trees and are often kept under natural vegetation. The Calcic Cambisols are generally permeable and their vegetation is variable; it is often herbaceous with shrubs or used as croplands depending on the location. The Chromic Cambisols, without limestone and clay content, are more present at the surface than at depth. Their parent materials are generally impermeable or give impermeable decomposition products. Podzolic soils present three differentiated acidic horizons, the deepest being the horizon of accumulation of clay and iron. The near-surface layers are light colored ones where they leach iron and organic matter from their upper horizons to lower horizons, creating dark subsurface horizons. They support shrubs, grassland and trees with little wood.

The major land use/land cover classes are croplands (with 66% of area), dense and open forests of Oak cork, shrublands and barren lands. Forests are found mainly on poorly developed soils on sandstone and conglomerate. Shrubs (Oleo-lentiscus and Erica europa) with an open canopy are often damaged by livestock and fires during the summer season. Overgrazing is observed in pasture and open shrubland. The Saf Saf watershed belongs to a temperate and humid climate of the Mediterranean type. The distribution of annual rains shows significant irregularities with a slightly fresh winter and a hot dry summer. Based on recorded daily rainfall of the 45-year period, the Saf Saf basin is characterized by a mean annual rainfall of 663 mm and a mean annual temperature of 21°C. Abundant rainfall values occur from November to April but storm events, exceeding 30 mm day^{-1}, are frequent from September to December.

3. Materials and methods

Data collection

The required data for this study are collected from different sources and the various types of data and satellite imagery are mainly topographic sheets, soil map, satellite data images and rainfall data. The research has involved integration of different thematic layers such as land cover map, DEM, rainfall, and soil map in GIS environment. The rainfall datasets, collected from 8 stations within the study basin, are used to develop the rainfall erosivity map (Fig. 1). Information on lithology is extracted from one 1:50,000 geological maps of Smendou, El Aria and Hammam Meskoutine that covers the study area. The Digital elevation model (30 m resolution) for the watershed is provided from the USGS National Map and NRCS Geospatial Data Gateway.

Soil data are relatively scarce and result largely from a soil map of Constantine at a scale of 1:200,000 developed by Durand (1954) and Digital Soil Map of the World (2007) produced by FAO-UNESCO (1:5,000,000 scale). Both maps are prepared to generate soil erodibility (K) map. Land cover and land use maps are realized using satellite imageries of Landsat-8 from 2019 and Google Earth Professional images at high resolution. Substantial amount of field data are collected to support image classification and validation.

RUSLE parameter estimation

RUSLE is becoming a method widely used around the world to predict long-term rates of soil erosion (Ganasri, and Ramesh, 2016; Tadesse et al., 2017). Moreover, it has demonstrated its time effectiveness to map and analyze erosion input data. A performed graphical user interface computer makes RUSLE easily used by integrating physically database input values that are widely available (Renard et al., 1997; Djoukbala et al., 2018; Fayas et al., 2019). Application of the RUSLE model has the advantages as its data require simple computational inputs available within a developing country like Algeria; it is compatible with GIS and it is easy to apply and understand from a functional approach (Wischmeier, and Smith 1978; Gupta, and Kumar, 2017). The RUSLE model can be expressed as equation (1):

$$A = R \times K \times LS \times C \times P \quad (1)$$

where A is the computed soil loss per unit area per year (t $ha^{-1}yr^{-1}$), LS is the slope length and steepness factor (dimensionless), K is the soil erodibility factor (t ha MJ^{-1} mm^{-1}), R refers to the rainfall erosivity factor (MJ mm ha^{-1} h^{-1} yr^{-1}), C is the land cover and management factor (dimensionless) and P is the support practice factor or the soil conservation (dimensionless). The calculation of the above-mentioned parameters is described in more detail below.

Rainfall erosivity factor (R)

The rainfall erosivity factor (R) represents the effect of rainfall intensity and frequency on soil erosion. R is defined as the product of storm kinetic energy and maximum 30-min intensity (EI30) (Arnoldous, 1978; Koirala et al., 2019). R-factor triggers erosion by the action of runoff and rainfall on soil surface (Abdul Rahaman et al., 2015).

Due to the lack of the rainfall intensity data within the study area, the equation developed by Wischmeier, and Smith (1978) is utilized. The parameter involves only annual and monthly precipitation to determine the R factor with the following equation:

$$R=\sum_{1}^{12} 1.753\times 10^{(1.5\log(Pi/P)-0.08188)} \quad (2)$$

where R is the annual rainfall erosivity factor (MJ mm ha^{-1} h^{-1} per year), P is the mean annual precipitation in mm, Pi is the mean monthly precipitation in mm.

For applying the above equation, the seasonal rainfall data is required. Daily data of rainfall from 1975 to 2017 are collected and average

rainfall data for used weather stations, located in the watershed are computed (Fig. 1). These rainfall point data are then interpolated using Inverse Distance Weighted (IDW) interpolation method by GIS technique in order to generate the rainfall distribution map and then the rainfall erosivity factor map. The inverse distance-weighted (IDW) interpolation analysis is chosen because the calculation process is simpler and easier to understand. Based on some authors (El-Zeiny, and Elbeih, 2019; Paul et al., 2019), the IDW is even precise as compared to kriging and has good accuracy.

Soil erodibility factor (K)

Soil erodibility is considered as a key parameter to measure soil susceptibility to water erosion. The soil erodibility factor (K) depends on the soil characteristics and the ability of soil or surface material to resist toerosion or to be removed by the rainfall/ runoff forces (Asmamaw, and Mohammed 2019; Fayas et al., 2019; Jazouli et al., 2019). The main soil properties influencing the K parameter aresoil permeability, organic matter content, soil texture and structure (Bou-imajjane et al., 2020; Yang et al., 2018).

The K-factor is determined by a simple method using the soil map of Constantine published by the Geographical Service of the Army in 1924 and updated in 1948, with a scale of 1:200,000. We can distinguish from the map four types of soil: Unsaturated soils, Calcareous soils, Podzolic soils and Solonetz Calcareous. With the help of Arcgis 10.4 version, the later map is georeferenced and the registered soil map is digitized and different soil attributes are assigned to the four soil groups according to the study catchment shapefile. The soils with their formerly names are renamed in relation to the FAO classification, with Chromic Cambisols (for unsatured soils), Calcic Cambisols (for Calcareous soils) and Orthic Solonetz (for Solonetz Calcareous). The Podzolic soil (or Podzols) name stayed unchanged because it exists in the classification system of the FAO soil groups.

Based on FAO-ISRIC (Food and Agriculture Organization of the United Nations International Soil Reference and Information Centre), the database DSMW (Digital Soil Map of the World) is imported into Arcgis10.4 in order to extract the four soil characteristics and generate the soil erodibility map. In order to determine the soil erodibility, the formula of Williams (1995) is adopted that has been widely used by several researchers (Chikh et al., 2019; Kateb et al., 2020). The used equation for K determination is as follows:

$$K = f_{csand} \times f_{cl\text{-}sil} \times f_{orgC} \times f_{hisand} \quad (3)$$

with f_{csand}: is a factor that represents low soil erodibility factors for soils with high coarse-sand contents and high values for soils with little sand; $f_{cl\text{-}sil}$: is a factor that reflects low soil erodibility factors for soils with high clay-silt ratios; $f_{org}C$: is a factor that reduces the erodibility for soils with high organic carbon content; f_{hisand} is a factor that reduces soil erodibility for soils with extremely high sand contents.

where:

$$f_{csand} = \left[0.2 + 0.3\exp\left(-0.0256\,ms\left(1-\frac{msil}{100}\right)\right)\right] \quad (4)$$

$$f_{cl\text{-}si} = \left[\frac{msil}{mcl + msil}\right]^{0.3} \quad (5)$$

$$f_{orgC} = \left[1 - \frac{0.25\,orgC}{orgC + \exp(3.72 - 2.95\,orgC)}\right] \quad (6)$$

$$f_{hisand} = \left[1 - \frac{0.70\,SN1}{SN1 + \exp(-5.51 + 22.9\,SN1)}\right] \quad (7)$$

with: ms: is the sand fraction content (0.05–2.00mm of diameter) in percent; msil: is the silt fraction content (0.002–0.05mm of diameter) in percent and mcl: is the clay fraction content (<0.002mm diameter) in percent; orgC: is the soil organic carbon (SOC) content (%) and SN1 = 1- (ms/100).

Topographic factor (LS)

The required RUSLE model is calculated through the combined topographic factor LS by using Digital Elevation Model. The Shuttle Radar Topography Mission (STRM) DEM

data is used in this present study. The DEM represents the bare-Earth surface, removing all natural (such as forest) and built features; therefore, in forested areas, DEM represents the height of trees in the area above ground-level. The STRM has 30-m resolution and improved accuracy (Maqsoom et al., 2020). The procedure of LS involves the steps for the creation of the slope (S) and length of slope (L) where both parameters represent the effect of topography on erosion .

The method is firstly conducted by generating slope and flow-accumulation map using the Spatial Analyst toolbox of Arcgis software. Secondly, the procedure is followed by the computation of LS-factor using a raster layer in GIS environment for each raster cell in a DEM, and by treating each pixel as its own segment of uniform slope (Bagherzadeh, 2014).

To estimate the LS-factor, SAGA GIS is used as it includes numerous applications such as those focused on DTMs (Digital Terrain Model), hydrology and terrain analysis. In SAGA GIS a module exists for calculating the LS-factor and furthermore gives a per-field function, which may limit the calculations to particular land parcels (additional input of polygon data). The slope map created with SAGA GIS and LS-factor are suitable for investigating slope lengths which can be taken into account in landscape management. At locations with large catchment area and narrow flow path combined with steep slope gradient the LS-factor and hence the erosional effect is high.

A slope map is created with the Slope, Aspect, Curvature tool of SAGA, using 9parameters and a 2nd degree polynomial as proposed by Zevenbergen, and Thorne (1987). To generate collection area or flow accumulation, the Flow Accumulation tool is used. In SAGA there are three different algorithms for calculating the LS factor. In thisproject the original equation of Wischmeier, and Smith (1978) is used, implemented in SAGA, which incorporates a multiple flow algorithm to estimate the flow accumulation (Panagos et al., 2015). The empirical equation developed by Wischmeier, and Smith (1978) is provided by the following formula:

$$LS = \left(\frac{L}{22.13}\right)^{m} \times (0.065 + 0.045 * S + 0.0065 * S^{2} \quad (8)$$

where L is the slope length in meters, S is the angle of slope in percent, m is a constant dependent on the value of the slope gradient: 0.5 if the slope angle is greater than 5%, 0.4 on slopes of 3% to 5%, 0.3 on slopes of 1 to 3%, and 0.2 on slopes less than 1%. The method of using flow accumulation, upslope contributing area, and slope in a GIS environment has gained in popularity due to its ability to principally account for convergence-divergence criterion of flow, thus catching more complex terrains (Benavidez et al., 2018).

Cover management factor (C)

Vegetation cover is regarded as one of the most important factor that influences the magnitude of soil loss caused by water; meanwhile, the C-factor is the one that helps policy makers and farmers to help for crop management. Since C-factor is not available for most of Algerian crops, it is used to indicate the effect of cropping and management practices on vulnerable agricultural lands to soil erosion. The importance and effects of plant cover on controlling soil erosion in forested regions vary with season and crop production system (Ganasri, and Ramesh, 2016).The rate of soil erosion often varies within the different vegetation cover and crop management practices (Esa et al., 2018).

For this study, Landsat 8 image is acquired on 29 December 2019 with a spatial resolution of 30 m. Various digital image-processing techniques to obtain valuable information related to the study area are used to identify the classes and feature. Using ERDAS Imagine 9.1 software, the data are loaded in the computer to create land use map. Geometric rectification of the data is carried out with the help of Survey of Saf Saf Toposheets

watershed for assigning geographical coordinates to keep pixel of the image. In this classification system of land use/land cover different categories have been taken, because remote sensing and GIS techniques are able to give us broad tool for better identification and analysis. The classes which have been identified and different LULC (land use/ land cover) layers are created. For this study; supervised type of classification is used with the known ground truth points by connecting ERDAS Imagine with Google Earth and synchronizing the images. The classification process is controlled by creating, managing, evaluating, and editing signatures using the Signature Editor.

The classification of satellite image is performed with a set of target classes in mind. Such a set is called a classification system. The purpose of such a system is to provide a framework for organizing and categorizing the information that can be extracted from the data. In this study, the total classification is achieved with the supervised method. The objective of the ERDAS Imagine software is to enable us to iteratively create and refine signatures and classified image files to arrive at a desired final classification. The process of classification, using ERDAS Imagine, is distinguished as an example by signatures that are created from supervised training. The signature evaluation tools can be used to indicate which signatures are spectrally similar. This helps to determine which signatures should be merged or deleted. These tools also help in defining optimum band combinations for classification that may reduce the time required to run a classification process or pixels' classification in function of signatures.

In addition, the classification by maximum likelihood (MLC) is used which performs a classification on an input image layer using a signature file. We calculate for each pixel of the image its probability of being attached to one class rather than another. The resulting assignment rule makes it possible to minimize the risk of error. The maximum likelihood classification requires: i- a choice of zones taken as references (the nuclei); ii- a statistical and radiometric analysis of these nuclei; iii- the study of the separability and performance tables. The final product of this work is the land use map composed of 6 themes: forest, shrub, grassland, cropland, barren land, urban area. The accuracy of image classification is checked using ground control points to represent the land use according to the specific land cover types.

Taking into account the realized land use map, the tables established by Wischmeier, and Smith (1978) and results of previous studies carried out in the Mediterranean region (Sadiki et al., 2009; El Garouani et al., 2008; Lahlaoi et al., 2015), and based on the height of the vegetation as well as the vegetation cover rate, we have given each type of ground cover a specific value. Each land use example, C values assigned through reference ranges from 0 to 1, where lower C means no loss, while higher indicates uncover and significant chances of soil loss (Panagos et al., 2015). Based on the tables of C-factors assigned to each land use from the above mentioned studies, the specific value ranges from 1 on barren soil where losses are intensified, to 0.13 under degraded forests, to 0.30 under sparse herbaceous vegetation and 0.60 with croplands given the crop calendar where the soil is left without vegetation protection during the wettest months (El Hage Hassan et al., 2018). The value higher than 0.4 indicates the least covered surface and in the case of croplands of the study area there is no conservation management practices such as diversified crop rotations. Factor C decreases to 0.07 under shrubs, which may provide continuous protection with less degraded cover.

Conservation practice factor (P)

The conservation practice factor (P) represents the ratio of soil loss in a field with specific support practice to the corresponding loss of soil under conditions of up and down slope tillage (Alewell et al., 2019). The value of P-factor ranges from 0 to 1 (0 indicates good conservation practice and

1 represents poor conservation practice). In this research, P is set equal to one across the watershed because there are no erosion-control works in the basin to prevent soil erosion and farmers do not use conservation tillage practices and contour ploughing.

4. Results and discussion

Results

Factor of rainfall erosivity (R)

The result of IDW interpolation using precipitation data of 8 meteorology stations over a 43-year period have shown that the mean annual rainfalls of the watershed are ranging from 560.20 to 625.40 mm with the highest value in the northern part of the watershed. The rainfall erosivity map based on annual data indicates that the R-factor value of the watershed is ranging from 21 to 58 MJ mm $ha^{-1}yr^{-1}$ (Fig. 2) with higher values occurring in the west part of the watershed, and the potential of rainfall to erode soil gradually decreases toward the east and southeast part of the watershed. The mean annual value of R is equal to 39.70MJ mm h^{-1} yr^{-1}.

Fig. 2. shows that the high degree of aggressiveness is observed mainly upstream of Bou Hadjeb Wadi from Bir ed Dzaria Hill (northwest area) to Beni Oufline (southwest area); the upper Khemakhem sub-basin including Ouled Habeba area is showing the least affected area by rainstorms. The low to moderate R values (21 to 43 MJ mm h^{-1} yr^{-1}) occupy 63.68% of the basin area.

In general, the variation in rainfall intensity is probably due to variation in elevation and exposure, where the elevations vary from 657 m to 1112 m. Moreover, the rainfall erosivity is surely directly proportional to the amount of rainfall received in different parts of the river basin.

Factor of soil erodibility (K)

The major soil types in the watershed are Calcic Cambisols, Chromic Cambisols, Podzoloc soils, and Orthic Solonetz, with the largest areas (42% and 32.47%) occupied by Orthic Solonetz and Chromic Cambisol soil types respectively.

The spatial distribution of the erodibility using geostatistical Analyst in Arcgis shows four different layers of the K-factor (Fig. 3). It ranges from 0.0138 to 0.0185 t ha MJ^{-1} mm^{-1} in areas. The lowest value of erodibility (0.0138) accounts for about 41% of the watershed and corresponds to Calcic

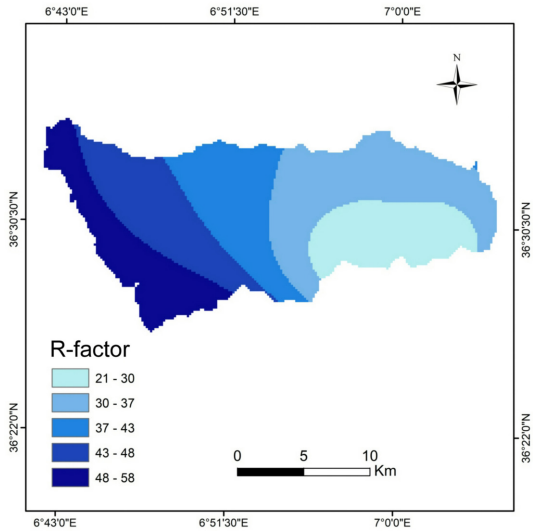

Fig. 2. Rainfall erosivity distribution of Saf Saf watershed

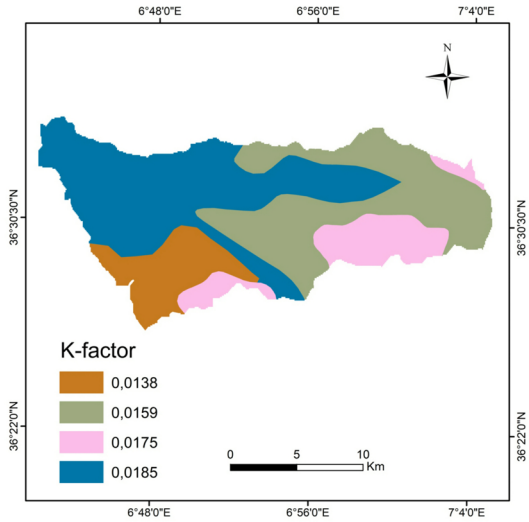

Fig. 3. Soil erodibility factor distribution of Saf Saf watershed

Cambisols (BK) dominated by sand (82%), covering mainly sandstone formation. The soil is characterized by low levels of organic matter, silt and clay levels. This type of texture gives the soil good macroporosity and permeability.

The highest soil erodibility with K value equal to 0.0185 accounts for about 42% of the watershed. It is defined by Orthic Solonetz that comprises soil with about 58% sand content, 29% clay content, and about 14% silt content (Table 1). The geology of this area is made of gypsiferous clay, calcareous and clayey limestone, and marly limestone. The present texture of the soil having low permeability is associated with erodible rocks, which means that this type of soil has reduced infiltration capacity and tends to compact on the surface, resulting in pore closure and the formation of a surface crust and hence high erodibility (Porta Casanellas et al., 2003). This high K value encourages soil erosion to occur.

The intermediate values of K represent the Podzolic soils and the Chromic Cambisols. The texture of these soils is mainly sandy and silty, but with a higher content of clay in the chromic Cambisols and higher organic carbon levels in the Podzolic soils.The fairly high percentage of clay found in the Chromic Cambisols can be considered as more optimal for balanced and fertile soils. However, its clay content may be a key in playing a role in increasing soil erodibility.

The spatial distribution of the K-factor shows that the most erodible soils (K > 0.017) are located on slopes with broad class ranges from 3% to > 25%. Land use found in

Table 1. Soil properties and K factor estimation

Soil unit symbol	sand (%) topsoil	silt (%) topsoil	clay (%) topsoil	OC (%) topsoil	f_{csand}	$f_{cl\text{-}sil}$	f_{orgC}	f_{hisand}	K
BC	40.10	21.50	38.4	1.44	0.20	0.36	0.82	1.00	0.016
Bk	81.60	6.80	11.70	0.44	0.20	0.37	0.99	0.72	0.014
P	69.50	23.90	6.70	3.86	0.20	0.78	0.75	0.95	0.018
So	57.60	13.50	29.00	0.39	0.20	0.32	0.99	1.00	0.019

BC: Chromic Cambisols; Bk: Calcic Cambisols; P: Podzolic soils; So : Othic Solonetz ; K-value unit: t ha MJ^{-1} mm^{-1}

Table 2. Statistical results of LS factor in the study area

LS class	MIN	MAX	STD	Basin area (km^2)
0 - 5	0.07	5.00	1.40	49.30
5 - 10	5.00	10.00	1.43	69.00
10 - 15	10.00	15.00	1.44	61.65
15 - 25	15.00	25.00	2.84	73.47
> 25	25.00	58.00	19.12	66.25

MIN : minimum ; MAX : maximum ; STD : standard deviation

the area is mostly of degraded shrubs and croplands in the western part; nevertheless, the moderate to high soil erodibility (0.014 < K < 0.017) is observed also in areas of degraded forest and shrubs, associated with grasslands (mainly in southeastern part). The lowest K value is dominated by a less accentuated topography where sandstone and clay outcrops are dominant, essentially covered by forest and shrubs.

Factor of Topography (LS)

The length and slope of each segment are measured and the LS-factor for each segment is computed using RUSLE method and Arcgis. It is known that the LS-factor varies throughout the watershed depending on the existing C and P factors (Chadli, 2016), but generally, the steeper the slopes and flow accumulation the higher is the LS-factor. The slope percentage ranges between 0 and 58% in the study area, where the LS standard deviation has reached high value in some places, indicating a significant difference in the topographic status of the area (Table 2). A mean value of LS-factor is equal to 17.59.

The LS class of low values represents the low slopes (0-5%) and characterizes more than 49% of the total basin area. The high values (LS > 15%) represent almost 44% (Table 2), that it is observed throughout many surfaces in the basin where the relief is high (Fig. 4).

According to the existing topography of the basin, the soils are classified as prone to rill or interrill erosion, where 63% of the study area has slopes exceeding 15%.There is generally a threshold length at which rilling will start

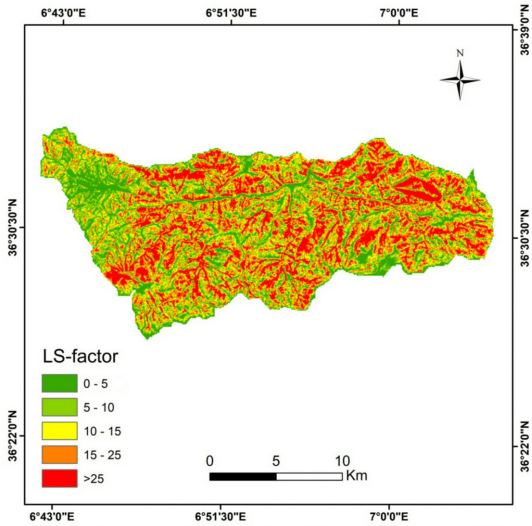

Fig. 4. Length-slope (LS) factor of Saf Saf watershed

to occur especially since runoff usually varies with steepness more on low slopes but not on steep slopes (Angima et al., 2003).

Factor of cover management (C)

The C-factor represents the positive effects of the vegetation cover on the soil particles stability and thus the soil losses reduction, by their actions characterized in the kinetic energy absorption of raindrops and the decrease in runoff; for this reason, each land cover type can correspond to an estimated C value (Boufeldja et al., 2020). The cereal crop may contribute in the deterioration of biomass and crop yields due to removal of nutrients for plant growth by continuous sheetwash and rills over the land surface.

Information on land use permits a better understanding of the land utilization aspects of cropping pattern, forest, wasteland and surface water bodies, which are vital for developmental planning/erosion studies in stopping or reducing soil erosion. Remote sensing and GIS technique has a potential to generate a thematic layer of land use-land cover of a region (Ganasri, and Ramesh, 2016).

The study area is classified into six land use classes (Fig. 5). Crop management factor is assigned to different land use patterns using the values from 0 (urban area) to 1 (bare soil), with a mean value of 0.28. Using land use-land cover map and C-factor value, the C-factor map is created.

The spatial distribution of C-factor shows that the most sensitive area to soil erosion is located in the northwestern part of the study area with less permanent vegetation cover such as cultures, where 15.40% of the watershed area has C values equal to 0.60. The high C-factor results usually from variation of vegetation cover throughout the year during the rainy seasons (Fall and Winter). Consequently, the sensitivity to soil erosion is different from one season to another. The fairly high C-factor (value of 0.30) is characterized by sparse grasslands that are undergoing sheetwash and rill erosion. They are distributed as smaller extensions throughout the basin, which represent 24.24% of the basin area.

The moderate C values occupy almost 53.60%of the basin area. The area is distinguished by mainly shrubs (C = 0.07) and sparse forest (C = 0.13) developed in the north at Bou Aded and Sesnou hillslopes and south at Beni Oufline and Ouled Habeba.

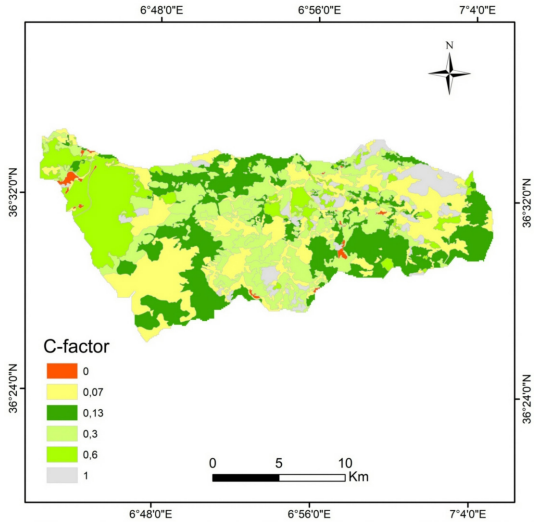

Fig. 5. Map of cover management factor of Saf Saf watershed

Assessment of potential soil erosion

The soil loss map of Saf Saf watershed is produced in GIS by multiplying the five factor parameters. The individual layers of the factors of RUSLE (R, K, LS, C and P) are created and combined together by a modeling procedure in the grid defined by ArcGIS 10.4 environment. The soil loss is calculated for each pixel of the grid.

The value of soil loss generated from the soil loss thematic map ranges from 0 to 117 t ha^{-1} yr^{-1} with mean value of 3.29 t ha^{-1} yr^{-1} and coefficient of variation of 1.03. The highest value of 34323.3 does not represent the overall soil loss but it represents the value of one pixel only. The high value pixels are mainly shown in areas of barren land, some agricultural lands and built-up areas and also in areas where the topography is highly dissected with steep slopes (Fig. 6). Therefore, current surfaces are found to be more affected and sensitive in terms of soil erosion.

Soil loss values have been grouped into seven classes based on the rate of erosion (Table 3). Out of the total area of Saf Saf waterhsed, 65.90% (211 km^2) falls under slight soil erosion zone where the potential soil erosion is between 0 and 2.5 t ha^{-1} yr^{-1}. As shown in Table 3, 85.26% of the Saf Saf watershed area has soil erosion rates values in the range 0 - 5 t ha^{-1} yr^{-1}, which can be classified as slight to slight-moderate vulnerability (e.g. soil erosion intensity),

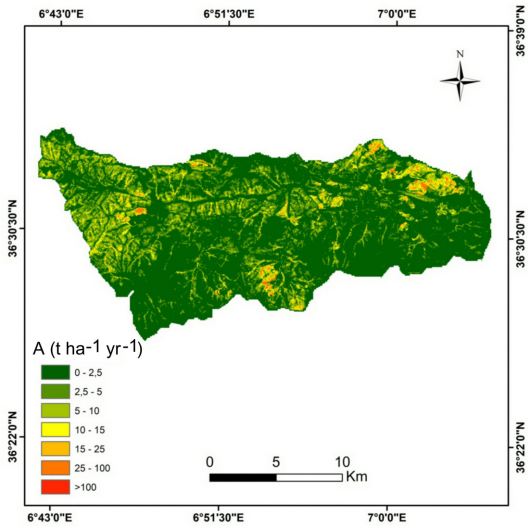

Fig. 6. Map of soil losses for Saf Saf river watershed

Table 3. Classes and intensity of soil losses in Saf Saf watershed according to Beskow et al. (2009)

Soil loss classes (t ha^{-1} yr^{-1})	Erosion intensity	Basin Area (Km^2)	Basin Area (%)
0 – 2.5	Slight	211	65.90
2.5 - 5	Slight to moderate	62	19.36
5 - 10	Moderate	32.38	10.11
10 - 15	Moderate to high	8.17	2.55
15 - 25	High	4.65	1.45
25 - 100	Very High	1.89	0.59
>100	Extremely high	0.08	0.02

10.11% of the area has values ranging from 5 to 10 t ha^{-1} yr^{-1}, characterizing these regions of the watershed as moderate vulnerability, and 4.00% of the basin shows soil losses between 10 and 25 t ha^{-1} yr^{-1}, which can be considered as high vulnerability. The high to extreme soil loss area represents only 0.61% of the basin with a value higher than 25 t ha^{-1} yr^{-1}.

Discussion

In this study, multiple data such as image satellite, DEM data, soil map, and rainfall data are integrated with the RUSLE model to estimate potential soil loss of Saf Saf watershed. In this study, validation of the model output is challenging due to poorly available input soil data. However, as an alternative, the consistency of the model stays an estimated approach to future developed studies on soil erosion.

The amount of potential soil erosion in the Saf Saf river basin is estimated at about 4.53 million tonnes with a maximum loss of 117 t ha-1 yr-1. As USLE-type model is designed to predict long-term average annual soil loss, it has been successful to predict event soil losses reasonably well for the study basin; however, one of the biggest limitations of USLE/RUSLE is the lack of estimation of connectivity within the watershed. Thus, this amount is the potentially detached soil of which ~80% would be deposited within the basin. Therefore the actual, net soil loss from the basin (considered as a summary) would be lower by orders. There is no simulation of soil deposition and that in most cases not enough measured data exist to rigorously determine the single factors for all needed situations and scenarios (Wischmeier, and Smith, 1978, p. 58).

In Algeria, no classification of soil loss is announced. Some researchers have indicated that the tolerable soil loss threshold cannot be more than 5 t ha-1 yr-1 (Prasannakumar et al., 2012). An adapted classification has been established in the United States based on the tolerance of loss in soils, where soil loss tolerance limits in current use in the USA vary between 4.5 and 11.2 t ha^{-1} yr^{-1} (Mannering, 1981). These values are based on soil depth, state of erosion and other factors which affect productivity. This assumes on average that soils can tolerate loss up to 7.41 t ha^{-1} yr^{-1}, while allowing a high level of agricultural production (Sahli et al., 2019). For soil losses beyond 20 t ha^{-1} yr^{-1}, soils are severely degraded, which is to affect vegetation state of health and sustainability.

Although Saf Saf watershed is experiencing the lowest soil erosion compared to other territories, with soil loss tolerance set less than 7 t ha^{-1} yr^{-1} for more than 85% of basin area, there is still the need for sustainable planning to protect the natural resources. Planners should focus mainly on very high and high soil erosion hotspot territories.

The spatial pattern of classified soil erosion risk zones indicates that the high levels of soil erosion risk zones are spatially correlated with steepest slopes, active streamflow courses and areas with low vegetation cover, which are much more located in the upstreams of Bou Adjeb and Khemakhem wadis and south of the watershed (Fig. 6). It should be noted that these parts are essentially affected by moderate to high erodibility. Also, these areas are distinguished by steep slopes (LS ≥ 15) that are able to increase runoff velocity for eroding and transporting more soil particles downslope. This fragility associated with Chromic Cambisol and Orthic Solonetz soils that are not enough protected by vegetation (C > 0.30) which denotes the greatest vulnerability and highest fragility of the study area to soil erosion. The lowest values of erosion risk are found in densely covered zones by shrubs and forest despite steeper slopes in some areas or in flat agriculture lands.

The grassland and unprotected agricultural land are land cover categories (39.28% of area) that contribute a lot to the total soil loss in the watershed. In the same order, they are responsible for more than 35% of the total soil loss. The closed forest followed by the

shrubs is the land cover which shares less soil erosion loss.

The findings are correlated with high hazards prediction in Algeria, where natural and man-induced factors lead to the degradation of the natural environment, thus initiating the change occurred of many natural geo-hazards, including the soil erosion. Some results have been found in the northeastern part of Algeria having similar geo-environmental conditions, absence of sustainable erosion control, and where human intervention has been mentioned to be among the major factors that accelerate the pressure to natural ecosystem; thus increase the soil erosion. For instance, the recent estimated soil loss of 286 t ha^{-1} yr^{-1} is outlined in Jijel (Algeria) by Nehaï, and Guettouche (2020), and many other authors such as Bouhadeb et al. (2018) and Sahli et al. (2019) have reported the role of human action in disturbing the soil stability. At the levels of Bounamoussa and Soummam watersheds, both located in the northeast of Algeria, the authors have reported average soil losses of 8 and 7 t ha^{-1} yr^{-1} respectively.

Consequently, the RUSLE method has given results approaching those carried out with a study on the same watershed using measurements of instantaneous suspended sediment concentrations and water discharges at its outlet (e.g. Khemakhem hydrometric station) for the period 1976 to 2014. The estimated mean annual sediment yield is found to be equal to 4.77 t ha^{-1} yr^{-1} (Khanchoul et al., 2019). Moreover, it should be noted that the RUSLE model only predicts surface soil erosion and does not takes into account channel bank erosion, which can be a very important sediment source in the study watershed (Khanchoul et al., 2007). The estimated sediment yield values may be improved with the inclusion of a bank erosion factor, although this would accentuate the already estimated values of the modelled sediment yields.

Nevertheless, it is noteworthy to notice that the difference between the results may be attributed to the difference in soil conditions, topography and the support practice as well as the difference in methods of estimation and/or the factors associated with them. In this territory like others, the erosion hazard is accentuated by a lack of soil erosion control; as a result, contributed significantly to accelerate runoff downslope. Consequently, droving high soil erosion which in turn, accelerates the land degradation and soil nutrient deprivation, and a decline in agricultural yield leads to food insecurity in the basin. Hence, conservation appears to be the most important factor to reduce the rate of runoff and prevent soil erosion under steep cultivated areas (Panagos et al.,2015; Kulimushi et al., 2021).

5. Conclusion

The results presented in this study have shown that it is possible to use a modelling RUSLE approach to develop a detailed spatial assessment of the distribution of erosion risk across the Saf Saf watershed and to highlight the responsible factors.

The overall potential soil erosion is estimated at 3.29 t ha^{-1} yr^{-1}, which is nearly lesser than the tolerable rate of 5t ha^{-1} yr^{-1}. The basin experiences soil losses estimated between 0 and 117 t ha^{-1} $year^{-1}$. The results obtained show that the study area is represented mainly by low to moderate soil loss rates ranging from 0 to 5 t/ha/year (with 85% of area), which is much lower than the tolerated threshold. The high loss rates are spread over 4% of the study area mainly in the northeast, northwest and south where topographic indices are high. The estimated amount of soil loss leads to the point that the watershed presents a low to moderate erosion risk.

Although these values are based on a given vegetation cover which may vary seasonally and from a year to another, they show the high range of sensitivity of the basin to water erosion. The present study can be improved seasonally using several vegetation cover maps to investigate the sensitivity of the soil

losses.

Most of the agriculture fields and sparse grasslands located near the river sides must follow very serious and effective conser¬vation practices. The reforestation of unstable and degraded parts of the south and north regions should be reinforced to stabilize existing erosion forms and barren land should be used sustainable with some alternative cultivation practices.

6. References

Abdul Rahaman, S.- Rahaman, S.A.- Aruchamy, S.- Jegankumar, R.- Ajeez, S.A. (2015): Estimation of annual average soil loss; based on RUSLE model in Kellar watershed, Bhavani basin, Tamil Nadu, India, ISPRS", Annals of Photogrammetry, Remote Sensing and Spatial Information Sciences II-2/W2: 207–214.

Angassa, A. (2014): Effects of grazing intensity and bush encroachment on herbaceous species and rangeland condition in Southern Ethiopia, Land Degradation and Development 25(5): 438–451.

Angima, S.D.- Stott, D.E.- O'Neill, M.K.- Ong, C.K.- Weesies, G.A. (2003): Soil erosion prediction using RUSLE for central Kenyan highland conditions, Agriculture, Ecosystems and Environment 97: 295–308.

Alewell, C.- Borrelli, P.- Meusburger, K.- Panagos, P. (2019): Using the USLE: Chances, challenges and limitations of soil erosion Modelling, International Soil and Water Conservation Research 7(3): 203–225.

Arnoldous, H.M.J. (1978): An approximation of the rainfall factor in the USLE in assessment of erosion. Wiley, Chichester, England.

Asmamaw, L.B.- Mohammed, A.A. (2019): Identification of soil erosion hotspot areas for sustainable land management in the Gerado catchment, North-eastern Ethiopia, Remote Sensing Applications: Society and Environment,13: 306–317.

Bagherzadeh, A. (2014): Estimation of soil losses by USLE model using GIS at Mashhad plain, Northeast of Iran, Arabian Journal of Geosciences 7: 211–220.

Benavidez, R. - Jackson, B. - Maxwell, D. - Norton, K. (2018): A review of the (Revised) Universal Soil Loss Equation (RUSLE): with a view to increasing its global applicability and improving soil loss estimates, Hydrology and Earth System Sciences 22: 6059–6086.

Beskow, S.- Mello, C.R.- Norton, L.D.- Curi, N.- Viola, M.R.- Avanzi, J.C. (2009): Soil erosion prediction in the Grande River Basin, Brazil using distributed modeling, Catena 79(1): 49–59.

Boufeldja, S.- Baba Hamed, K.- Bouanani, A.- Belkendil, A. (2020): Identification of zones at risk of erosion by the combination of a digital model and the method of multi-criteria analysis in the arid regions : Case of the Bechar Wadi watershed, Applied Water Science 10(5): 121.

Bouhadeb, C.E.- Menani, M.R.- Bouguerra, H.- Derdous, O. (2018): Assessing soil loss using GIS based RUSLE methodology. Case of the BouNamoussa watershed – North-East of Algeria, Journal of Water and Land Development 36(1): 27–35.

Bou-imajjane, L.- Belfoul, M.A.- Elkadiri, R.- Stokes, M. (2020): Soil erosion assessment in a semi-arid environment : A case study from the Argana Corridor, Morocco, Environmental Earth Sciences 79(18): 409.

Chadli, K. (2016): Estimation of soil loss using RUSLE model for Sebou watershed (Morocco), Modeling Earth Systems and Environment 2:51.

Chikh, H.A.-Habi, M.-Morsli, B. (2019): Influence of vegetation cover on the assessment of erosion and erosive potential in the Isser marly watershed in northwestern Algeria - Comparative study of RUSLE and PAP/RAC methods, Arabian Journal of Geosciences 12(5): 154.

Digital Soil Map of the World. (2007): Geonetwork. http://www.fao.org/geonetwork/srv/en/-metadata.show%3Fid=14116.

Djoukbala, O.- Mazour, M.- Hasbaia, M.- Benselama, O. (2018): Estimating of water erosion in semiarid regions using RUSLE equation under GIS environment, Environmental Earth Sciences 77(9): 345.

Durand, J.H. (1954): Les sols d'Algérie, Gouvernement Général de l'Algérie, Direction du Service de la Cartographie et de l'Hydraulique. Service des Etudes Scientifiques, Pédologie, n° 2, Alger. 244.

El Garouani, A.- Chen, H.- Lewis, L.- Tribak, A.- Abahrour, M. (2008): Cartographie de l'utilisation du sol et de l'érosion nette à partir d'images satellitaires et du SIG Idrissi au nord-est du Maroc, Revue Télédétection 8(3): 193–201.

El Hage Hassan, H.- Charbel, L.-Touchart, L. (2018): Modélisation de l'érosion hydrique à l'échelle du bassin versant du Mhaydssé,Békaa-Liban, VertigO 18(1).

El Jazouli, A.- Barakat, A.- Ghafiri, A.- El Moutaki, S.- Ettaqy, A.- Khellouk, R. (2017): Soil erosion modeled with USLE, GIS, and remote sensing : A case study of Ikkour watershed in Middle Atlas (Morocco), Geoscience Letters 4(1): 25.

El-Zeiny, A.M.- Elbeih, S.F. (2019): GIS-based evaluation of groundwater quality and suitability in Dakhla Oases, Egypt, Earth Systems and Environment 3: 507–523.

Esa, E.-Assen, M.-Legass, A. (2018): Implications of land use/cover dynamics on soil erosion potential of agricultural watershed, northwestern highlands of Ethiopia, Environmental Systems Research 7(1): 21.

Fang, G.- Yuan, T.- Zhang, Y.- Wen, X.- Lin, R. (2019): Integrated study on soil erosion using RUSLE and GIS in Yangtze River Basin of Jiangsu Province (China), Arabian Journal of Geosciences 12: 173.

FAO.(2015): Global soil status, processes and trends. Status of the World's Soil Resources (SWSR). Main Report of the Food and Agriculture Organization, New York, United Nations.

Fayas, C.M.- Abeysingha, N.S.- Nirmanee, K.G.S.- Dinithi Samaratunga, D.- Mallawatantri, A. (2019): Soil loss estimation using rusle model to prioritize erosion controlin Kelani river basin in Sri Lanka. International Soil and Water Conservation Research 7: 130–137.

Ganasri, B.P.- Ramesh, H. (2016): Assessment of soil erosion by RUSLE model using remote sensing and GIS - A case study of Nethravathi Basin, Geoscience Frontiers 7(6), 953–961.

Gupta,S.- Kumar, S. (2017): Simulating climate change impact on soil erosion using RUSLE model - A case study in a watershed of mid-Himalayan landscape, Journal of Earth System Science 126: 43.

Haregeweyn, N.- Tsunekawa, A.- Nyssen, J.- Tsubo, M.- Meshesha, D.T.- Schutt, B.-Adgo, E.- Tegegne, F. (2015): Soil erosion and conservation in Ethiopia: a review, Progress in Physical Geography 39(6): 750–774.

Jazouli, A.E.- Barakat, A.- Khellouk, R.- Rais, J.- Baghdadi, M.E. (2019): Remote sensing and GIS techniques for prediction of land use land cover change effects on soil erosion in the high basin of the Oum ErRbia River (Morocco), Remote Sensing Applications: Society and Environment 13: 361–374.

Kateb, Z.- Bouchelkia, H.- Benmansour, A.- Belarbi, F. (2020): Sediment transport modeling by the SWAT model using two scenarios in the watershed of Beni Haroun dam in Algeria, Arabian Journal of Geosciences 13(14): 653.

Khanchoul, K.- Jansson, M.B.- Lange, J. (2007): Comparison of suspended sediment yield in two catchments, northeast Algeria, Zeitschrift für Geomorphogie 51(1): 63–94.

Khanchoul, K.- Boukhrissa, Z.A. (2019): Assessing suspended sediment yield in the Saf Saf gauged catchment, northeastern Algeria, Malaysian Journal of Geosciences 3(2): 01–05.

Koirala, P.- Thakuri, S.- Joshi, S.- Chauhan, R. (2019): Estimation of soil erosion in Nepal using a RUSLE modeling and geospatial tool, Geosciences 9: 147.

Kouli, M.- Soupios, P.- Vallianatos, F. (2009): Soil erosion prediction using the Revised Universal Soil Loss Equation (RUSLE) in a GIS framework, Chania, Northwestern Crete, Greece, Environmental Geology 57: 483e497.

Kulimushi, L.C.- Choudhari, P.- Mubalama, L.K.- Banswe, G.T. (2021): GIS and remote sensing-based assessment of soil erosion risk using RUSLE model in South-Kivu province, eastern, Democratic Republic of Congo, Geomatics, Natural Hazards and Risk 12(1): 961–987.

Lahlaoi, H.- Rhinane, H.- Hilali, A.- Lahssini, S.- Khalile, L. (2015): Potential erosion risk calculation using remote sensing and GIS in Oued El Maleh watershed, Morocco, Journal of Geographic Information System 7: 128–139.

Mannering, J.V. (1981): The use of soil loss tolerances as a strategy for soil conservation. In: Morgan, R. P. C. (ed.) Soil conservation. Problems and Prospects, pp. 337-350, John Wiley, Chichester.

Maqsoom, A.- Aslam, B.- Hassan, U.- Kazmi, Z.A.- Sodangi, M.-Tufail, R.F.- Danish Farooq, D. (2020): Geospatial assessment of soil erosion intensity and sediment yield using the Revised Universal Soil Loss Equation (RUSLE) model, International Journal of Geo-Information 9(6): 356.

Napoli, M.- Cecchi, S.- Orlandini, S.- Mugnai, G.- Zanchi, C.A. (2016): Simulation of field-measured soil loss in Mediterranean hilly areas (Chianti, Italy) with RUSLE, Catena 145: 246–256.

Nehaï, S.A.- Guettouche, M.S. (2020): Soil loss estimation using the revised universal soil loss equationand a GIS-based model: a case study of JijelWilaya, Arabian Journal of Geosciences 13(4):152.

Panagos, P.- Borrelli, P.- Poesen, J.- Ballabio, C.- Lugato, E., - Meusburger, K.- Montanarella, L.- Alewell, C. (2015): The new assessment of soil loss by water erosion in Europe, Environmental Science and Policy 54: 438–447.

Panagos, P.- Imeson, A.- Meusburger, K.- Borrelli, P.- Poesen, J.- Alewell, C. (2016c): Soil conservation

in Europe: Wish or reality? Land Degradation and Development 27(6): 1547–1551.

Paul, R.- Brindha, K.- Gowrisankar, G.- Tan, M.L.- Singh, M.K. (2019): Identification of hydrogeochemical processes controlling groundwater quality in Tripura, Northeast India using evaluation indices, GIS, and multivariate statistical methods, Environmental Earth Sciences 78(15): 1–16.

Prasannakumar, V.- Vijith,H.- Abinod,S.- Geetha, N. (2012): Estimation of soil erosion risk within a small mountainous sub-watershed in Kerala, India, using Revised Universal Soil Loss Equation (RUSLE) and geo-information technology, Geoscience Frontiers 3(2): 209–215.

Porta Casanellas, J.- López-Acevedo Reguerín, M.- Roquero de Laburu, C. (2003): Edafología: para la agricultura y el medio ambiente Edaphology to the agriculture and environment. World press editions. 929.

Prasannakumar, V.- Vijith, H.- Abinod, S.- Geetha, N. (2012): Estimation of soil erosion risk withina small mountainous sub-watershed in Kerala, India, using Revised Universal Soil LossEquation (RUSLE) and geo-information technology, Geoscience Frontiers 3(2): 209–215.

Rawat, K.S.- Mishra, A.K.- Bhattacharyya, R. (2016): Soil erosion risk assessment and spatial mapping using LANDSAT-7 ETM+, RUSLE, and GIS–a case study, Arabian Journal of Geosciences 9(4): 1–22.

Renard, K.- Foster, G.- Weesies, G.- McCool, D.- Yoder, D. (1997): Predicting soil erosion by water: a guide to conservationplanning with the Revised Universal Soil Loss Equation (RUSLE), Agricultural Handbook 703: 65–100.

Sadiki, A.- Faleh, A.- Zêzere, J.L.- Mastass, H. (2009): Quantification de l'érosion en nappes dans le bassin versant de l'oued Sahla Rif central Maroc, Cahiers Géographiques 6: 59–70.

Sahli, Y.- Mokhtari, E.- Merzouk, B.- Laignel, B.- Vial, C.- Madani, K. (2019): Mapping surface water erosion potential in the Soummam watershed in Northeast Algeria with RUSLE model, Journal of Mountain Science 16(7): 1606–1615.

Shi, P.- Zhang, Y.- Ren, Z.- Yu, Y.- Li, P.- Gong, J.(2019): Land-use changes and check dams reducing runoff and sediment yield on the Loess Plateau of China, Science of the Total Environment 664: 984–994.

Stefanidis, S.- Alexandridis, V.- Chatzichristaki, C.- Stefanidis, P. (2021): Assessing soil loss by water erosion in a typical mediterranean ecosystem of Northern Greece under current and future rainfall erosivity,Water 13: 2002. https://doi.org/10.3390/w13152002.

Sun, C.- Hou, H.- Chen, W. (2021): Effects of vegetation cover and slope on soil erosion in the Eastern Chinese Loess Plateau under different rainfall regimes, PeerJ 9: e11226 http://doi.org/10.7717/peerj.11226.

Tadesse, L.- Suryabhagavan, K.V.- Sridhar, G.- Gizachew, L. (2017): Land use and land cover changes and soil erosion in Yezat watershed, north western Ethiopia, International Soil Water Conservation Research 5: 85–94.

Toumi, S. (2013): Application des techniques nucléaires et de la télédétection a l'étude de l'érosion hydrique dans le bassin versant de l'Oued Mina. Thèse de Doctorat Es-Sciences, l'Ecole Nationale Supérieure d'Hydraulique, Algérie.175.

Teixeira Guerra, A.J.- Fullen, M.A.- Oliveira Jorge, M.D.C.- Rodrigues Bezerra, J.F.-Shokr, M.S. 2017. Slope processes, mass movement and soil erosion: a review, Pedosphere 27(1): 27–41.

Williams, J.R. (1995): Chapter 25: The EPIC model. In: Singh, V.P. (ed.): Computer models of watershed hydrology, Water Resources Publications 909–1000.

Wischmeier, W.H.- Smith, D.D. (1978): Predicting rainfall erosion losses - a guide to conservation planning, agriculture. Handbook No, 537, USDA/Science and Education Administration, US, Govt, Printing Office, Washington D.C.

Yang, X.- Gray, J.- Chapman, G.- Zhu, Q.- Tulau, M.- McInnes-Clarke, S. (2018): Digital mapping of soil erodibility for water erosion in New South Wales, Australia, Soil Research 56 : 158–170.

Yjjou, M.- Bouabid, R.- El Hmaidi, A.- Essahlaoui, A.- El Abassi, M. (2014): Modélisation de l'érosion hydrique via les SIG et l'équation universelle des pertes en sol au niveau du bassin versant de l'Oum Er-Rbia, The International Journal of Engineering and Science 3(8): 83–91.

Zevenbergen, L.W.- Thorne, C.R. (1987): Quantitative analysis of land surface topography, Earth Surface Processes and Landforms 12: 47–56.